

Pseudomonas putida KT2440 response to nickel or cobalt induced stress by quantitative proteomics†

Cite this: *Metallomics*, 2013, 5, 68

Prasun Ray,^{ab} Vincent Girard,^{ab} Manon Gault,^{ab} Claudette Job,^{ab} Marc Bonneau,^c Marie-Andrée Mandrand-Berthelot,^{ab} Surya S. Singh,^d Dominique Job^{ab} and Agnès Rodrigue^{*ab}

Nickel and cobalt are obligate nutrients for the gammaproteobacteria but when present at high concentrations they display toxic effects. These two metals are present in the environment, their origin being either from natural sources or from industrial use. In this study, the effect of inhibitory concentrations of Ni or Co was assessed on the soil bacterium *Pseudomonas putida* KT2440 using a proteomic approach. The identification of more than 400 spots resulted in the quantification of 160 proteins that underwent significant variations in cells exposed to Co and Ni. This analysis allowed us to depict the cellular response of *P. putida* cells toward metallic stress. More precisely, the parallel comparison of the two proteomes showed distinct responses of *P. putida* to Ni or Co toxicity. The most striking effect of Co was revealed by the accumulation of several proteins involved in the defense against oxidative damage, which include proteins involved in the detoxification of the reactive oxygen species, superoxides and peroxides. The up-regulation of the genes encoding these enzymes was confirmed using qRT-PCR. Interestingly, in the Ni-treated samples, *sodB*, encoding superoxide dismutase, was up-regulated, indicating the apparition of superoxide radicals due to the presence of Ni. However, the most striking effect of Ni was the accumulation of several proteins involved in the synthesis of amino acids. The measurement of the amount of amino acids in Ni-treated cells revealed a strong accumulation of glutamate.

Received 3rd January 2012,
Accepted 28th November 2012

DOI: 10.1039/c2mt20147j

www.rsc.org/metallomics

Introduction

Nickel and cobalt are trace elements widely utilized by organisms. In gammaproteobacteria, comparative genomic analyses showed that the majority of sequenced bacteria of this phylum are equipped with genes involved in the metabolism of Ni or Co.¹ Ni enzymes fulfill nine different biological processes, the best characterized ones being hydrogenase and urease.² Co is either a co-factor in itself or utilized by enzymes in the form of cobalamin (vitamin B12).³ A set of accessory proteins is necessary to ensure proper metal concentration within the cell. These are specific uptake systems, chaperones, regulatory proteins and efflux systems. Uptake systems as well as efflux pumps often

transport both Ni and Co. These are for example the importer proteins of the NiCoT family exemplified by HoxN⁴ or the efflux pumps of the RND or RcnA families.^{5,6} By reason of their close chemical properties Ni and Co are often bound by the same protein. Ni and Co are present in the natural environment. Ni is found as a major constituent of serpentine soils for instance. It is admitted that both metals occur jointly in the environment.⁷ They are used in the metallurgical industry for the production of stainless steel for instance. Due to their extensive use, considerable amounts of Ni or Co are present in the aquatic environment or in biological wastewater treatment plants and are retrieved in sewage sludge or solid waste composts.⁸

Pseudomonas putida is a ubiquitous gram-negative soil bacterium belonging to the gamma class of *Proteobacteria*. Genomic analysis revealed that *P. putida* KT2440 harbours a large variety of genes predicted to be involved in metal homeostasis or resistance⁹ with a great proportion of genes being present in genomic islands,¹⁰ inferring that this bacterium thrives in heavy metal contaminated environments. However, the molecular mechanisms of metal tolerance or resistance are poorly described in this bacterium.

The harmful effects of Ni and Co in prokaryotes have been understudied and still need to be investigated. The deleterious

^a Université de Lyon, Lyon, F-69003, INSA Lyon, Université Lyon 1, Villeurbanne, F-69621, France

^b Microbiologie, Adaptation et Pathogénie, UMR 5240 CNRS-UCBL-INSA-BCS, Bat. Lwoff, 10 rue Dubois, Villeurbanne Cedex, F-69622, France.

E-mail: agnes.rodrigue@insa-lyon.fr; Fax: +33 472431584; Tel: +33 472447980

^c Plate-forme Protéomique, Université Bordeaux 2, Bordeaux, France

^d Department of Biochemistry, Osmania University, Hyderabad, India

† Electronic supplementary information (ESI) available. See DOI: 10.1039/c2mt20147j

effect of Co seems to be due mainly to the inactivation of iron-sulfur clusters present in enzymes and to the inhibition of the Fe-S cluster assembly process.¹¹ The aim of the present study was to analyze the cell response to inhibitory concentrations of Ni or Co in *P. putida* KT2440 by quantitative proteomics. The parallel investigation of the effect of the two metals allowed us to unveil the specific response to each metal.

Material and methods

Bacterial strain and culture conditions

P. putida KT2440 was cultivated in M63 minimal medium supplemented with 0.4% succinate as the carbon source. For the estimation of bacterial doubling time cells were grown in 250 mL Erlenmeyer flasks with 25 mL medium without metal or amended with 75 μM NiSO₄ or 35 μM CoCl₂ with orbital shaking (150 rpm) at 30 °C. Cell growth was monitored based on culture optical density at 600 nm (A_{600}). The doubling time was estimated by the equation: $g = (\log_{10} N_t - \log_{10} N_0) / \log_{10} 2$, where N_t = natural log of the number of cells (A_{600}) at time t and N_0 = natural log of the number of cells (A_{600}) at time zero.

Protein sample preparation

Bacteria were grown under the above conditions and were harvested in the logarithmic growth phase ($A_{600} \approx 2.00$). Cell pellets were obtained by centrifugation (10 000 $\times g$ for 15 min). The pellets were briefly washed in 10 mM tris-HCl (pH 8.0) and were lysed by three passages in a French press at 1000 psi. The debris were removed by centrifugation (10 000 $\times g$ for 15 min), and the lysate was centrifuged at 30 000 $\times g$ for 2 h to separate the soluble and membrane fractions. The soluble proteins were quantified by the standard Bradford assay (BioRad). Bovine serum albumin was used as a standard. The protein samples were precipitated (TCA/acetone) and stored frozen at -80 °C.

Two-dimensional gel electrophoresis

An amount of 25 μg of protein was used for analytical gels, while an amount of 40 μg of protein was used for the preparative gels. Isoelectric focusing (IEF) of protein extracts in rehydration buffer (8 M urea, 4% [w/v] CHAPS, 0.5% [v/v] IPG buffer, pH 3–10, 40 mM DTT, and 0.01% [w/v] bromophenol blue) was run using 24 cm immobilized pH gradient (3–10 nonlinear) IPG strips on the PROTEAN[®] IEF system (BIORAD). Strips were rehydrated for 20 h at 22 °C with the thiourea/urea lysis buffer containing 40 mM DTT and the protein extracts. Isoelectrofocusing was performed at 20 °C for 30 min at 100 V, 30 min at 250 V, 30 min at 1000 V, and 5 h at 7000 V.¹² IEF strips were equilibrated for 2 \times 20 min in 2 \times 100 ml of equilibration solution containing 6 M urea, 37.5% (w/v) glycerol, 2.5% (w/v) SDS and tris-HCl (0.04 M pH 8.8). DTT 2% (w/v) was added to the first equilibration solution and iodoacetamide 2.5% (w/v) was added to the second.

Equilibrated gel strips were placed on top of vertical 12% polyacrylamide gels. A denaturing solution containing 1% (w/v) low-melting agarose, 0.03% (w/v) Trizma-base, 1.4% (w/v) glycine, and 0.25% [w/v] SDS was loaded on gel strips.

After agarose solidification, electrophoresis was performed at 10 °C in Laemmli buffer (pH 8.3), for 1 h at 35 V and 110 V overnight. Ten gels were run in parallel (Isodalt system from Amersham Pharmacia Biotech).¹² For each condition, analyzed 2-D gels were made at least in triplicate and for a minimum of three independent extractions.

Protein staining and gel analyses

2-D gels were stained with silver nitrate¹³ using the Hoefer Automated Gel stainer apparatus from Amersham Pharmacia Biotech. Analytical silver-stained gels were scanned with the Sharp JX-330 scanner equipped with the Labscan version 3.00 from Amersham Pharmacia Biotech. After spot detection and background subtraction (mode: average on boundary), 2D gels were compared, matched, and the quantitative determination of the spot volumes was performed (mode: total spot volume normalization). For each analysis, statistical data showed a high level of reproducibility between normalized spot volumes of gels produced in triplicate. Data were subjected to statistical analysis by using Student's t test ($\alpha = 0.05$).¹²

The quantitative results herein described have been obtained from 494 spots for which a systematic quantification was performed, based on spot intensity, by comparing different conditions (without metal or amended with 75 μM Ni or 35 μM Co) with three gels per condition. For calibrating molecular weight and pI scales of 2D gels, commercial standard (GE, Serva and Pierce) was used.

In-gel digestion of proteins and sample preparation for MS analysis: data acquisition and database searching

For protein identification, 379 spots showing different levels of intensity were excised from 2D gels manually. Gel pieces were destained using the PROTSIL2 kit (Sigma-Aldrich, St. Louis, MO). Spots were rinsed twice in ultrapure water and shrunk in acetonitrile (ACN) for 10 min. After ACN removal, gel pieces were dried in a vacuum centrifuge and rehydrated in 10 ng μL^{-1} trypsin solution (Sigma-Aldrich) in 50 mM ammonium bicarbonate and incubated overnight at 37 °C. Hydrophilic peptides were extracted with 40 mM ammonium bicarbonate containing 10% (v/v) ACN at room temperature for 10 min. Hydrophobic peptides were extracted with 47.0% ACN, 5% (v/v) formic acid and the extraction step was repeated twice. All three supernatants were pooled together, concentrated in a vacuum centrifuge, and acidified with 0.1% formic acid.¹⁴ For MALDI TOF MS/MS analyses, a volume of 0.5 μL of each sample was spotted onto a Prespotted AnchorChip target plate (Part No. 231968, Bruker) according to the manufacturer's instructions. Mass spectrometry analyses were performed on an Ultraflex III TOF/TOF (Bruker, Bremen, Germany) in positive ion reflector mode.¹⁴ Mass spectra were acquired over the m/z range 450–5000 and were subsequently externally calibrated against adjacent spots prespotted with the peptide calibration mixture (PAC_PeptideCalibStandard, Bruker). 1500 and 300 shots were usually accumulated for MS and MS/MS spectra, respectively. MS/MS precursor ions were selected depending on Peptide Mass Fingerprint results (see below): in the case of PMF success, three out of the most intense ions were selected for MS/MS confirmation and

five unidentified ions were selected for MS/MS exploration. In the case of PMF failure, MS/MS experiments were performed on the eight most intense ions from the MS spectra. For LC-ESI-MS/MS analyses, peptide mixtures were analyzed using an on-line capillary nano-HPLC (LC Packings, Amsterdam, Netherlands) coupled to a nanospray LCQ Deca XP ion trap mass spectrometer¹⁴ (ThermoFinnigan, San Jose, CA, USA). Peptide digests (10 μL) were loaded onto a 300 μm inner diameter \times 5 mm C18 PepMapTM trap column (LC Packings, Amsterdam, Netherlands) at a flow rate of 30 $\mu\text{L min}^{-1}$. The peptides were eluted from the trap column onto an analytical 75 μm inner diameter \times 15 cm C18 PepMapTM column (LC Packings, Amsterdam, Netherlands) with a 5–40% linear gradient of solvent B in 30 min (solvent A was 0.1% formic acid in 5% ACN, and solvent B was 0.1% formic acid in 80% ACN). The separation flow rate was set at 200 nL min^{-1} .¹⁴ The mass spectrometer operated in positive ion mode at a 2 kV needle voltage and a 3 V capillary voltage. Data acquisition was performed in a data-dependent mode alternating in a single run, a MS scan survey over the m/z range 150–2000, a zoom scan and a MS/MS scan of the most intense ion in the survey scan. MS/MS spectra were acquired using a 2 m/z unit ion isolation window at 35% relative collision energy and 0.5 min dynamic exclusion duration.

PMF spectra were searched with MASCOT 2.2 software (<http://www.matrixscience.com>) against the *P. putida* KT2440 JCVI database (5437 entries). Monoisotopic mass tolerance was set at 50 ppm, one trypsin-missed cleavage was allowed, and oxidation of methionine was considered as a variable modification and carbamido-methylation of cysteine as a fixed modification. A minimal Mascot score of 54 was set for protein identity validation. A tolerance of 0.7 Da in MS/MS mode was also considered for MS/MS spectra searches. Proteins were validated as soon as two different peptides were validated (individual ion scores > 20).¹⁴ Peptides from LC-MS/MS spectra were identified with the SEQUEST algorithm through Bioworks 3.3.1 interface (Thermo-Finnigan, Torrence, CA, USA) against the same *P. putida* KT2440 database used in MASCOT. DTA generation allowed the averaging of several MS/MS spectra corresponding to the same precursor ion with a tolerance of 1.4 Da. Spectra from precursor ions higher than 3500 Da or lower than 600 Da were rejected. The search parameters are as follows: mass accuracy of the peptide precursor and peptide fragments was set to 2 and 1 Da, respectively. Only b- and y-ions were considered for mass calculation. Oxidation of methionines and carbamidomethylation of cysteines were considered as differential modifications. Two missed trypsin cleavages were allowed. Trypsin peptides were validated using the following criteria ($\Delta\text{CN} \geq 0.1$, $X_{\text{corr}} \geq 1.9$ (single charge), 2.2 (double charge), 3.75 (triple charge), peptide probability ≤ 0.001). A minimum of two different peptides was considered for protein validation.¹⁴

Amino acids assay

We used the Agilent method for HPLC analysis of amino acids.¹⁵ Chromatographic analysis was achieved with an HPLC 1100 series equipped with a quaternary pump module (G1311A), an automatic sampler (G1329A) and a Diode Array

Detector (DAD G1315B) (Agilent Technologies). Before injection, 1 μL of samples was online-derivatized using orthophtalaldehyde (OPA) and 9-fluorenylmethyl chloroformate (FMOC). The separation was carried out at room temperature using a Zorbax Eclipse-AAA Column (4.6 \times 150 mm, 3.5 μm , Agilent Technologies). The column was eluted at 2 ml min^{-1} , with an optimized gradient established using solvents A (40 mM Na_2HPO_4 pH 7.8) and B (acetonitrile:methanol:water (45:45:10, v/v/v)). The used gradient was an increase of solvent B (0% to 57% in 8.8 min), then an increase of solvent B (57% to 100% in 0.2 min), and then isocratic conditions for 2 min. 3D data were recorded and specific wavelengths at 262 nm (secondary amino acids) and 338 nm (primary amino acids) were chosen for processing. The Chemstation Agilent software was used for integration and comparison of chromatograms. Each amino acid was quantified at an appropriate wavelength with a specific calibration curve.

cDNA synthesis and real-time PCR

Total RNA were isolated with the cold phenol method. Briefly, the bacteria were grown in M63 minimal medium or supplemented with 75 μM NiCl_2 or 35 μM CoCl_2 . Cells were broken mechanically in the presence of glass beads in a Fast Prep (MP) apparatus. RNA was extracted twice using a (25:24:1) mix of phenol/chloroform/isoamyl alcohol. RNA was ethanol precipitated and treated twice with DNase (Ambion) for 30 min at 37 $^\circ\text{C}$. The absence of DNA contamination was verified by direct PCR. RNA was quantified by measuring the optical density at 260 nm (OD260), and its integrity was confirmed by agarose gel electrophoresis. RNA was reverse-transcribed using the RevertAid kit (Fermentas). Real-time PCR experiments were performed using the MasterPLUS SYBRGreen I kit (Roche Applied Science). The 16S RNA gene was chosen as reference gene for data normalization. Amplification and detection of the specific products were carried out with the LightCycler System, and data analysis was performed with the Lightcycler Relative Quantification software (Roche Applied Science). Relative expression was calculated as the ratio of the normalized value of each sample relative to that of the corresponding untreated cells according to ref. 16.

Results and discussion

Ni or Co effect on the growth of *P. putida*

To assess the biological impact of challenging concentrations of Ni or Co on the growth of *P. putida* KT2440, the bacteria were grown in succinate minimal medium supplemented with increasing concentrations of one or the other metal added from the start of the culture. As expected, increasing concentrations of metals led to decreased cell growth. Under these conditions, Minimal Inhibitory Concentrations of 200 μM and 100 μM were obtained for Ni and Co respectively (Fig. S1, ESI[†]). For the present study, the chosen concentrations of Ni and Co were the ones resulting in an increase of about 30% of the average doubling time as compared to the growth in the absence of metal. In succinate supplemented minimal medium, the average doubling time measured was 100 min (Fig. 1). When 75 μM Ni or 35 μM Co were present, doubling times of 130 min

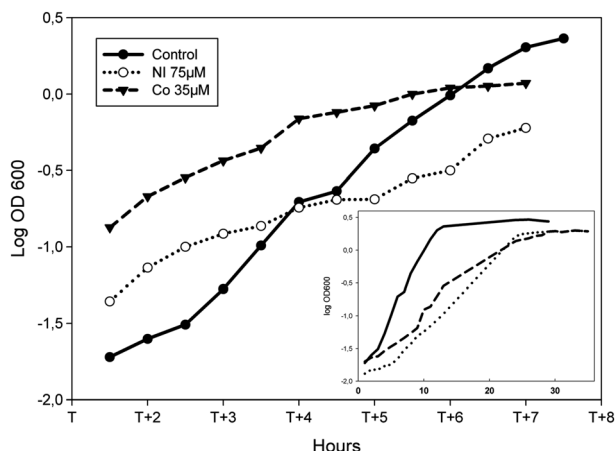


Fig. 1 Effect of Ni or Co on the growth of *P. putida* KT2440. Logarithmic representation of growth curves during the logarithmic phase of cells grown in minimal medium supplemented with 0.4% succinate (closed dots, plain line), amended with 75 μM NiCl_2 (open dots, dotted line) or 35 μM CoCl_2 (closed triangles, dashed line). X axis: T corresponds to the time the bacteria enter into logarithmic growth phase. Inset: the same growth curves are shown from the start of the culture to the late stationary phase.

and 140 min were measured respectively (Fig. 1). These doses, which are moderately cytotoxic, might activate both the specific cellular response as well as more general stress pathways. Interestingly, the parallel analysis of Ni or Co-treated proteome should give access to both types of information.

2-DE

The bacteria were grown in the above-referred concentrations, 75 μM Ni or 35 μM Co, until late logarithmic phase ($\text{OD}_{600} \approx 1.00$) and the soluble fraction of the total proteome was collected and analyzed by 2-DE. 2D-gels of protein extracts from cells grown in the absence of metal were compared with those from cells grown in the presence of 75 μM NiCl_2 or 35 μM CoCl_2 . According to the cumulative analysis of various gels, the software Labscan determined approximately 580 spots (Fig. 2). After PMF or LC-MS analysis, 483 proteins were identified.

Protein identification and annotation

Finally, the quantification of 160 different proteins was achieved that correspond to the analysis of the spots containing only one protein. 41 up-regulated and 72 down-regulated proteins in the Co-treated samples and 54 up-regulated proteins and 46 down-regulated proteins in the Ni-treated proteome constituted the dataset (Fig. 3, Tables 1 and 2). Quite interestingly, the set of commonly regulated proteins included 17 up-regulated and 36 down-regulated proteins (Table 3). Protein identification was made according to the JCVI *P. putida* KT2440 database (version 1.2). Annotation was achieved using a combination of information from Swissprot (and linked databases) and additional elements from the literature. The proteins were sorted manually into 11 major functional classes (Fig. 3 and Tables 1–3).

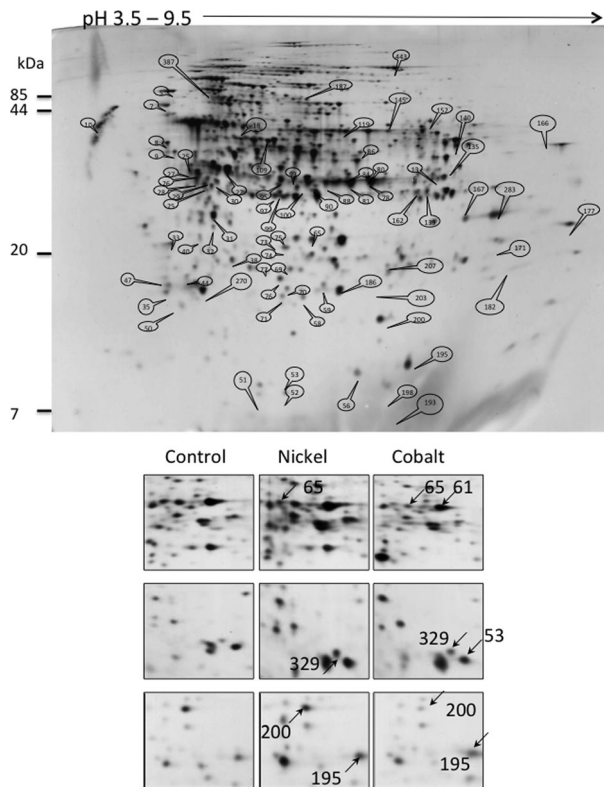


Fig. 2 2-DE analysis of the *P. putida* proteome. Upper panel: total gel image of a 12 h culture soluble proteome of *P. putida* KT2440 grown in minimal medium supplemented with succinate. Lower panel: proteome comparison after growth in the presence of 75 μM Ni or 35 μM Co. Examples of spots variation are shown. Spots 61: PP_0018, 65: PP_4185, 53: PP_4730, 195: PP_5156, 200: PP_4981, 329: PP_5414.

Comparison of Ni and Co effects unveils a common core of metal stress responsive proteins

Antioxidants. The two main classes of proteins whose level increased after treatment by both metals are “Antioxidants, detoxification” and “Protein synthesis” (Table 3). Thiol peroxidase (Tpx), PP_3587, and alkyl hydroperoxidoreductase, AhpC/Tsa family protein PP_1084, belong to the peroxiredoxin family, which are ubiquitous proteins that confer resistance to oxidative stress. These enzymes catalyze the reduction of hydrogen peroxide and a wide range of organic hydroperoxides to their corresponding alcohols.¹⁷ PP_4506 is annotated as a nitroreductase, a widespread family of enzymes whose primary function is to metabolize nitro-substituted compounds and that more generally are oxidoreductases. One nitroreductase, NfsA, was shown to reduce chromate to the less toxic form Cr(III) in *E. coli*, thus protecting cells against chromate toxicity.¹⁸ PP_2463 is classified as a CspA member of the Cold Shock Proteins (Csp) family. These proteins are known to be involved in the response to stress and have been shown to play a role in transcription and translation processes, in particular by acting as RNA chaperones thus enhancing the stability of mRNA transcripts.¹⁹ Recently *csp* gene family mutants of *Listeria monocytogenes* were shown to display higher oxidative stress sensitivity, which indicates that Csps are also involved in oxidative stress adaptation.²⁰ Surprising was the decreased level

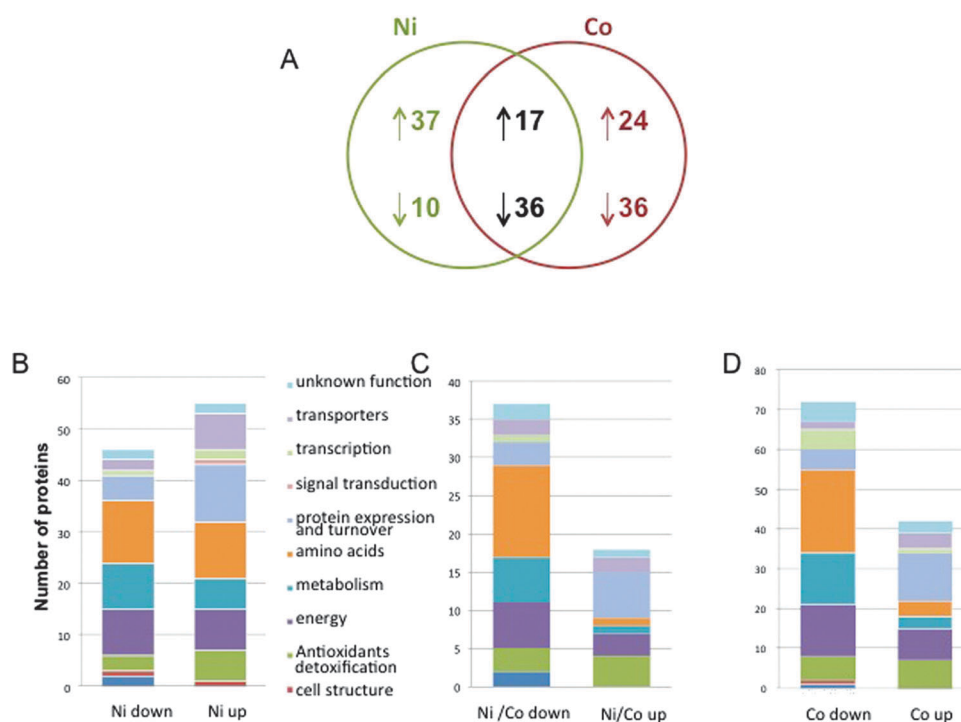


Fig. 3 *P. putida* proteome response to Ni and Co. (A) Venn diagram of common and unique sets of proteins expressed in cells exposed to Ni and Co. The diagram indicates the number of proteins whose synthesis was increased (upward arrow) or decreased (downward arrow) after metal exposure. (B) Functional classification of the Ni-specific proteome. (C) Functional classification of the Ni and Co common proteome. (D) Functional classification of the Co-specific proteome.

of MsrA (PP_0336). MsrA is a methionine sulfoxide reductase that reduces methionine sulfoxide back to methionine preventing protein oxidation. However, a second methionine sulfoxide reductase, MsrB (PP_1873), is present in the genome of *P. putida* KT2440 that might fulfill the function.²¹ The other explanation is that the defect in MsrA might contribute to the toxic effect of the metals. Taken together, our data strongly suggest that Ni and Co trigger oxidative stress in *P. putida*. This has been previously suggested for Co but was less clear for Ni in bacteria.²² One report indicated that cells of *P. putida* UW4 exposed to Ni produced several antioxidant proteins.²³

Protein synthesis. Another common core of proteins whose level increased in the Ni- and Co- treated samples was that of proteins involved in protein synthesis (Table 3). The increase of several ribosomal proteins (PP_0444, PP_0721, and PP_1772) and elongation factors (PP_0440, PP_1858) indicates the requirement for the cell to translate more proteins when Ni or Co is present. Considering the lower growth rate of the bacteria in the presence of these metals (Fig. 1), it can be assumed that enhanced protein synthesis is linked to the need for the cell to replace proteins that are damaged, e.g. by oxidation.

Amino acids metabolism. The main group of proteins that showed decreased accumulation upon Ni- or Co-treatment was the proteins involved in amino acid biosynthetic pathways (Table 3). More particularly, we identified proteins involved in the synthesis of amino acids from α -ketoglutarate, a Krebs cycle intermediate, namely glutamate, glutamine, arginine and proline.²⁴

The common precursor in proline and arginine synthesis is glutamine that is converted from glutamate by glutamine synthetase. Interestingly, several enzymes involved in the conversion of glutamate to arginine were present at a lower level: glutamine synthetase (*glnA*, PP_5046), acetylglutamate kinase (*argB*, PP_5289), *N*-acetylglutamate semialdehyde dehydrogenase (*argC1*, PP_0432), ornithine carbamoyl transferase (*argI*, PP_1000). In *P. putida* the catabolism of arginine can occur through four pathways.²⁵ In the present study the two arginine-catabolic pathways sharing glutamate as an end product were less expressed, namely in the arginine deiminase pathway, arginine deiminase (*arcA*, PP_1001) and ornithine carbamoyl transferase (*argI*, PP_1000) were repressed and in the arginine succinyltransferase pathway, the level of *N*-succinylarginine dihydrolase (*astB*, PP_4477) was decreased. Similarly, the synthesis of proline from glutamate seemed to be attenuated by reason of the decreased level of glutamine synthetase (*glnA*, PP_5046) and delta-1 pyrroline-5-carboxylate reductase (*proC*, PP_5095). These regulations conversely concur with the diminished synthesis of proline and arginine from glutamate. The genome of *P. putida* KT2440 possesses eight genes encoding glutamine synthetases (as deduced from the *P. putida* genome database).²¹ Under our conditions PP_5046 was found to be predominant and its level was diminished by Ni and Co. Glutamate is a key precursor involved in diverse metabolic pathways. Our data suggest that its use as a carbon source through the tricarboxylic acids (TCA) cycle is not favored under Ni or Co stress, as the level of aspartate ammonia lyase

Table 1 Differentially expressed proteins identified in *P. putida* KT2440 that were specifically regulated by Co treatment

Spot number	Co/Ctrl ^a	Accession no	Protein (gene) [EC] ^b	Functional classification	PI	MW, kDa
305	0.43	PP_1210	Ferritin Dps family protein	Antioxidants, detoxification	5.2	17.8
352	3.72	PP_0915	Fe superoxide dismutase (<i>sodB</i>) [1.15.1.1]	Antioxidants, detoxification	5.5	21.9
357	12.51	PP_1859	Organic hydroperoxide resistance protein (<i>ohr</i>)	Antioxidants, detoxification	6.28	14.8
354	16.34	PP_5215	Thioredoxin (<i>trx-2</i>)	Antioxidants, detoxification	4.9	11.7
82	3.10	PP_0842	Cysteine desulfurase (<i>iscS-1</i>) [2.8.1.7]	Antioxidants, detoxification	5.85	44.4
213	0.10	PP_0786	Thioredoxin reductase (<i>trxB</i>) [1.8.1.9]	Antioxidants, detoxification	5.22	34.0
37	2.44	PP_1638	Ferredoxin-NADP reductase (<i>fpr</i>) [1.18.1.2]	Antioxidants, detoxification	5.22	29.7
75	0.36	PP_4646	Ferredoxin-NADP reductase (<i>fprB</i>)	Antioxidants, detoxification	5.38	28.9
113_337	1.47	PP_5415	ATP synthase F1. Alpha subunit (<i>atpA</i>) [3.6.3.14]	Energy	5.38	55.5
324	0.22	PP_0072	Quinone oxidoreductase (<i>qor-1</i>) [1.6.5.5]	Energy: E-transfer	8.8	34.2
24	1.99	PP_5085	Malic enzyme (<i>maeB</i>) [1.1.1.40]	Energy: glyoxylate cycle	5.09	45.4
148	0.45	PP_1379	3-Carboxy- <i>cis,cis</i> -muconate cycloisomerase (<i>pcab</i>) [5.5.1.2]	Energy: protocatechuate degradation	6.08	48.4
341	4.79	PP_2334	Methylisocitrate lyase (<i>prpB</i>) [4.1.3.30]	Energy: TCA pathway	5.4	31.8
349	1.82	PP_2335	Methylcitrate synthase [2.3.3.5]	Energy: TCA pathway	6.3	42.0
125	0.11	PP_0944	Fumarate hydratase. Class II (<i>fumC-1</i>) [4.2.1.2]	Energy: TCA pathway	5.65	48.6
246_509	0.51	PP_4012	Isocitrate dehydrogenase, NADP-dependent, monomeric-type [1.1.1.42]	Energy: TCA pathway	5.44	80.1
132	0.61	PP_4187	2-Oxoglutarate dehydrogenase, lipamide dehydrogenase component (<i>lpdG</i>) [1.8.1.4]	Energy: TCA pathway	5.93	50.1
284	0.16	PP_4186	Succinyl-CoA synthetase, beta subunit (<i>succ</i>) [6.2.1.5]	Energy: TCA pathway	5.83	41.5
312	0.36	PP_3365	Acetolactate synthase, catabolic	Metabolism: energy/amino acids/nucleotides	5.75	60.3
85	0.33	PP_0671	Serine hydroxymethyltransferase (<i>ghA-2</i>) [2.1.2.1]	Metabolism: amino acids	5.85	45.1
276	0.08	PP_1471	Threonine synthase (<i>thrC</i>) [4.2.99.2]	Metabolism: amino acids	5.86	52.0
320	0.22	PP_0817	Aminotransferase, Class I	Metabolism: amino acids	8.7	45.0
212	0.21	PP_1237	Dihydrodipicolinate synthase (<i>dapA</i>) [4.2.1.52]	Metabolism: amino acids	5.73	31.9
433	0.25	PP_2371	Sulphite reductase hemoprotein, beta subunit (<i>cysI</i>) [1.8.1.2]	Metabolism: amino acids	5.5	62.2
321	0.52	PP_4473	Aspartate kinase (<i>lysC</i>) [2.7.2.4]	Metabolism: amino acids	5.25	44.7
211	0.37	PP_4571	Cysteine synthase A (<i>cysK</i>) [4.2.99.8]	Metabolism: amino acids	5.55	34.5
269	0.20	PP_4678	Ketol-acid reductoisomerase (<i>ihvC</i>) [1.1.1.86]	Metabolism: amino acids	5.48	36.6
314	0.22	PP_4680	Acetolactate synthase. Large subunit. Biosynthetic type (<i>ihvB</i>) [4.1.3.18]	Metabolism: amino acids	—	62.8
342	8.16	PP_2036	Dihydrodipicolinate synthase	Metabolism: amino acids	5.3	31.3
353	4.03	PP_3778	Pyrroline-5-carboxylate reductase	Metabolism: amino acids	5.8	27.7
345	3.77	PP_5155	D-3-phosphoglycerate dehydrogenase (<i>serA</i>) [1.1.1.95]	Metabolism: amino acids	5.9	44.3
147	0.32	PP_1362	Pyruvate kinase II (<i>pykA</i>) [2.7.1.40]	Metabolism: glycolysis	6.22	52.0
223	0.28	PP_1915	Acyl carrier protein (<i>acpP</i>)	Metabolism: lipid and sterol	4.11	8.7
234	0.20	PP_0558	Acetyl-CoA carboxylase, biotin carboxylase (<i>accC-1</i>) [6.4.1.2]	Metabolism: lipid and sterol	6.09	49.5
328	0.24	PP_4175	3-Oxoacyl-(acyl-carrier-protein) synthase I (<i>fabB</i>) [2.3.1.41]	Metabolism: lipid and sterol	5.3	43.2
471	0.56	PP_1457	Phosphoribosylglycinamide formyltransferase 2 (<i>purT</i>) [2.1.2.-]	Metabolism: nucleotides	5.61	42.8
264	0.24	PP_1610	CTP synthase (<i>pyrG</i>) [6.3.4.2]	Metabolism: nucleotides	5.61	59.8
418	2.15	PP_1179	Ribonucleoside reductase, alpha subunit (<i>nrdA</i>) [1.17.4.1]	Metabolism: nucleotides	5.5	106.9
225	0.24	PP_0776	Peptidyl-prolyl <i>cis-trans</i> isomerase, FKBP-type (<i>slyD</i>)	Protein destination and storage: folding and stability	—	17.2
47	1.89	PP_0684	Peptidyl-prolyl <i>cis-trans</i> isomerase, FKBP-type (<i>fkIB-1</i>) [5.2.1.8]	Protein destination and storage: folding and stability	4.64	21.7
12_13	1.31	PP_1361	Chaperonin, 60 kDa (<i>groEL</i>)	Protein destination and storage: folding and stability	4.97	56.7
8	1.92	PP_2299	Trigger factor (<i>tig</i>) [5.2.1.8]	Protein destination and storage: folding and stability	4.81	48.5
329	0.32	PP_4874	Ribosomal protein L9 (<i>rplI</i>)	Protein synthesis: ribosomal proteins	5.3	15.5
515	4.00	PP_0469	Ribosomal protein L6 (<i>rplF</i>)	Protein synthesis: ribosomal proteins	9.73	19.1
559	2.83	PP_1594	Ribosome recycling factor (<i>frr</i>)	Protein synthesis: translation factors	7.88	20.1
250_335	1.59	PP_1213	Aspartyl-tRNA synthetase (<i>aspS</i>) [6.1.1.12]	Protein synthesis: tRNA synthetases	5.34	66.9
226	0.21	PP_2084	Regulator of ribonuclease activity A (<i>rraA</i>)	Transcription: RNA fate	—	17.6
372_374	0.69	PP_4708		Transcription: mRNA processing	5	75.0

Table 1 (continued)

Spot number	Co/Ctrl ^a	Accession no	Protein (gene) [EC] ^b	Functional classification	PI	MW, kDa
			Polyribonucleotide nucleotidyltransferase (<i>pnp</i>) [2.7.7.8]			
406–412	0.26	PP_0447	DNA-directed RNA polymerase, beta subunit (<i>rpoB</i>) [2.7.7.6]	Transcription: mRNA synthesis	5.57	151.5
308	3.40	PP_0479	DNA-directed RNA polymerase, alpha subunit (<i>rpoA</i>) [2.7.7.6]	Transcription: mRNA synthesis	4.91	36.7
53	0.22	PP_4730	Transcriptional regulator Fur (<i>fur</i>)	Transcription: specific TFs	5.43	15.2
207	4.02	PP_0112	ABC transporter, periplasmic binding protein, putative	Transporters: ABC-type ^c	6.92	27.7
360	2.23	PP_1137	Branched-chain amino acid ABC transporter, ATP-binding protein (<i>braG</i>)	Transporters: ABC-type	7.7	25.5
282	0.48	PP_1826	Isochorismatase hydrolase	Unclear classification	7.05	21.5
171	0.15	PP_3249	Aldo/keto reductase	Unclear classification	7.81	29.6
61	0.07	PP_0018	Hypothetical protein	Unknown function	5.72	31.2
166	0.39	PP_0766	Hypothetical protein	Unknown function	9.17	50.5
195	0.53	PP_5156	Hypothetical protein	Unknown function	6.64	16.7
182	2.17	PP_3611	Hypothetical protein	Unknown function	9.07	20.8
198	4.65	PP_0998	Hypothetical protein	Unknown function	6.12	16.0

^a Ratio of protein abundance in the Co-treated cells to that in cells without metal. ^b Where available, the name of putative homologous gene is indicated in parentheses and the enzyme commission number is given in square brackets. ^c Transporters class: in this study the soluble proteome of *P. putida* was analyzed, which explains why transporter proteins were not identified apart from Periplasmic Binding Proteins (PBP) of the ABC transporter family that are soluble proteins.

(*aspA*, PP_5338) that catalyzes the conversion of aspartate to fumarate, the second step of the glutamate catabolism, was found to be significantly reduced (Table 3).

Central metabolism. Central metabolism was mainly affected in the TCA pathway, which is consistent with the growth on succinate as a carbon source utilized in this study. Pyruvate dehydrogenase (*aceE*, PP_0339) and aconitate hydratase 2 (*acnB*, PP_2339) were accumulated and may favor the formation of acetyl-CoA and isocitrate, respectively, whereas isocitrate dehydrogenase (*icd*, PP_4011), succinyl-CoA synthase (*sucD*, PP_4185) (see spot 65 in Fig. 2) and citrate synthase (*gltA*, PP_4194) were repressed. Since the TCA cycle is at the junction of the metabolism of sugars, proteins and lipids, its modulation is expected under stressful conditions.

The specific response to cobalt

Antioxidant defense – redox balance. The most striking response to the cobalt stress was the modulation of proteins involved in the defense against oxidative stress (Table 1). The protein displaying the highest level of accumulation in Co samples was thioredoxin (*trx-2*, PP_5215). Thioredoxin reduces disulfide bridges, which result from the oxidation of the –SH group in target proteins, resulting in the release of the reduced target and of oxidized thioredoxin.²⁶ Target proteins are for instance proteins of the peroxiredoxin family such as Tpx or Ohr that are regenerated upon reduction by thioredoxin. Interestingly, the level of Tpx was shown here to be increased by Ni and Co (see Table 3). In brief, the redox biology cycles of thiol-containing enzymes regenerate peroxiredoxin whose function is to reduce H₂O₂, fatty acid peroxides or organic peroxides.²⁶ Peroxiredoxins are reduced at the cost of oxidation of thioredoxins which in turn are reduced by thioredoxin reductase. *P. putida* KT2440, as many organisms, seems to contain only one thioredoxin reductase, TrxB (PP_0786), whose

level decreased in Co treated samples. This reduced level of TrxB might be the symptom of either altered stability of the protein due to damage or altered expression of the gene. To address this point, the expression of *trxB* was monitored at the mRNA level using RT-qPCR (see below). Oxidized thioredoxin reductases are reduced by NADPH. Ferredoxin-NADP reductases are critical for the maintenance of proper levels of NADPH inside cells. *P. putida* contains two of these enzymes whose expression is altered in opposite directions: the level of Fpr (PP_1638) increased whereas that of FprB (PP_4646) decreased. It has been recently shown that *fpr* regulation is under the control of FinR, a novel redox-sensing transcriptional regulator.²⁷

Another strongly enhanced protein was Ohr (organic hydroperoxide resistance protein, PP_1859), a hydroperoxidase with a clear preference for organic peroxides. The *in vivo* substrates are unknown but are thought to include lipid peroxides.²⁸ The anti-oxidative response is completed by Fe-superoxide dismutase (*sodB*, PP_0915) whose function is to scavenge superoxide O₂^{•-}. To depict a more complete picture of the thiol-redox biology in *P. putida* under metallic stress, the expression of *ohr* and *tpx* (peroxiredoxin), *trx-2* (thioredoxin), and *trxB* (thioredoxin reductase) was monitored at the mRNA level (see below).

Iron metabolism. Fur, the ferric uptake regulation protein, tightly controls the level of iron in the cell mainly by repressing iron uptake systems, to prevent excess iron from causing the apparition of reactive oxygen species (ROS) through the Fenton reaction. In the present study, the level of Fur (PP_4730) decreased five-fold upon Co treatment, suggesting increased iron acquisition. Most surprising was the down-regulation of Dps (PP_1210), a protein of the ferritin family that can act as an iron-storage protein as well as a non-specific DNA binding-protein, both functions concurring to the protection of the cell against stress.²⁹ Previous studies on *E. coli* demonstrated that Co interferes with iron homeostasis either by inducing iron

Table 2 Differentially expressed proteins identified in *P. putida* KT2440 that were specifically regulated by Ni treatment

Spot number	Ni/Ctrl	Accession no	Protein (gene) [EC]	Functional classification	PI	Mass
220	0.25	PP_1702	Recombination-associated protein (<i>rdgC</i>)	Cell growth/division	4.87	34.4
99	2.22	PP_1799	GDP-mannose 4.6 dehydratase (<i>gmd</i>) [4.2.1.47]	Cell structure: cell envelope	6	40.1
305	2.14	PP_1210	Ferritin Dps family protein	Antioxidants, detoxification	5.2	17.8
37	0.40	PP_1638	Ferredoxin-NADP reductase (<i>fpr</i>) [1.18.1.2]	Antioxidants, detoxification	5.22	29.7
33	2.46	PP_0538	Inorganic pyrophosphatase (<i>ppa</i>) [3.6.1.1]	Energy	4.77	19.2
324	4.05	PP_0072	Quinone oxidoreductase (<i>gor-1</i>) [1.6.5.5]	Energy: E-transfer	8.8	34.2
349	0.20	PP_2335	Methylcitrate synthase [2.3.3.5]	Energy: TCA pathway	6.3	42
460	0.42	PP_2337	Probable AcnD-accessory protein PrpF (<i>prpF</i>)	Energy: TCA pathway	5.31	41.3
246_509	2.63	PP_4012	Isocitrate dehydrogenase, NADP-dependent [1.1.1.42]	Energy: TCA pathway	5.44	80.1
132	1.28	PP_4187	2-Oxoglutarate dehydrogenase, lipamide dehydrogenase component (<i>lpdG</i>) [1.8.1.4]	Energy: TCA pathway	5.93	50.1
441_504	2.02	PP_4189	2-Oxoglutarate dehydrogenase, E1 component (<i>kgdA</i>) [1.2.4.2]	Energy: TCA pathway	6.1	106.9
38	0.51	PP_1389	Oxaloacetate decarboxylase [4.1.3.3]	Energy: TCA pathway	5.18	31.8
312	2.51	PP_3365	Acetolactate synthase, catabolic	Metabolism: energy/amino acids/nucleotides	5.75	60.3
85	2.40	PP_0671	Serine hydroxymethyltransferase (<i>glyA-2</i>) [2.1.2.1]	Metabolism: amino acids	5.85	45.1
533	7.73	PP_0675	Glutamate dehydrogenase (<i>gdhA</i>) [1.4.1.4]	Metabolism: amino acids	6.12	49.3
320	4.62	PP_0817	Aminotransferase, Class I	Metabolism: amino acids	8.7	45
212	2.80	PP_1237	Dihydrodipicolinate synthase (<i>dapA</i>) [4.2.1.52]	Metabolism: amino acids	5.73	31.9
433	1.91	PP_2371	Sulphite reductase hemoprotein, beta subunit (<i>cysI</i>) [1.8.1.2]	Metabolism: amino acids	5.5	62.2
321	14.70	PP_4473	Aspartokinase (<i>lysC</i>) [2.7.2.4]	Metabolism: amino acids	5.25	44.7
211	2.35	PP_4571	Cysteine synthase A (<i>cysK</i>) [4.2.99.8]	Metabolism: amino acids	5.55	34.5
269	2.15	PP_4678	Ketol-acid reductoisomerase (<i>ilvC</i>) [1.1.1.86]	Metabolism: amino acids	5.48	36.6
314	2.40	PP_4680	Acetolactate synthase, large subunit (<i>ilvB</i>) [4.1.3.18]	Metabolism: amino acids	—	62.8
133	3.96	PP_3511	Branched-chain amino acid aminotransferase (<i>ilvE</i>) [2.6.1.42]	Metabolism: amino acids	6.72	36.8
147	2.14	PP_1362	Pyruvate kinase II (<i>pykA</i>) [2.7.1.40]	Metabolism: glycolysis	6.22	52.05
234	2.10	PP_0558	Acetyl-CoA carboxylase, biotin carboxylase (<i>accC-1</i>) [6.4.1.2]	Metabolism: lipid and sterol	6.09	49.4
445	1.70	PP_4487	Acetyl-CoA synthetase 1 (<i>acsA1</i>) [6.2.1.1]	Metabolism: lipid and sterol	5.9	71.8
162	0.49	PP_4169	Glycerol-3-phosphate dehydrogenase (<i>gpsA</i>) [1.1.1.8]	Metabolism: lipid and sterol	6.2	36.5
375	2.91	PP_1031	Inosine-5-monophosphate dehydrogenase (<i>guaB</i>) [1.1.1.205]	Metabolism: nucleotides	6.5	51.8
274	0.41	PP_4889	Adenylosuccinate synthetase (<i>purA</i>) [6.3.4.4]	Metabolism: nucleotides	5.56	47.1
225	1.89	PP_0776	Peptidyl-prolyl <i>cis-trans</i> isomerase, FKBP-type (<i>slyD</i>)	Protein destination and storage: folding and stability	—	17.2
378	4.41	PP_4727	dnaK protein (<i>dnaK</i>)	Protein destination and storage: folding and stability	4.83	68.8
8	0.41	PP_2299	Trigger factor (<i>tig</i>) [5.2.1.8]	Protein destination and storage: folding and stability	4.81	48.5
329	3.48	PP_4874	Ribosomal protein L9 (<i>rplI</i>)	Protein synthesis: ribosomal proteins	5.3	15.5
42	3.65	PP_1592	Translation elongation factor Ts (<i>tsf</i>)	Protein synthesis: translation factors	5.14	30.4
260	0.53	PP_5044	GTP-binding protein Tya/BipA	Protein synthesis: translation factors	5.4	67.3
261	1.85	PP_2465	Threonyl-tRNA synthetase (<i>thrS</i>) [6.1.1.3]	Protein synthesis: tRNA synthetases	5.64	73.2
310	2.45	PP_0397	Putative serine protein kinase, PrkA	Signal transduction: kinases	7.74	74.0
226	2.15	PP_2084	Regulator of ribonuclease activity A (<i>rraA</i>)	Transcription: RNA fate	—	17.6
319	6.00	PP_5214	Transcription termination factor Rho (<i>rho</i>)	Transcription: general TFs	7.71	47.1
327	3.78	PP_0227	Amino acid ABC transporter, Periplasmic binding protein	Transporters: ABC-type	—	28.8
315	2.21	PP_0885	Dipeptide ABC transporter, periplasmic peptide-binding protein	Transporters: ABC-type	6.64	60.5
137	2.44	PP_3801	Cation ABC transporter, periplasmic cation-binding protein, putative	Transporters: ABC-type	6.67	32.8
89	2.31	PP_3558	Amino acid transporter, periplasmic amino acid-binding protein, putative	Transporters: ABC-type	5.6	36.9
170	2.37	PP_0824	Phosphate ABC transporter, periplasmic phosphate-binding protein, putative	Transporters: ABC-type	8.35	31.1
282	1.69	PP_1826	Isochorismatase hydrolase	Unclear classification	7.05	21.5
195	3.84	PP_5156	Hypothetical protein	Unknown function	6.64	16.7
198	0.55	PP_0998	Hypothetical protein	Unknown function	6.12	16.1

bioavailability depletion or by competing with iron for biological target sites.³⁰ In *P. putida*, Co could display comparable effects. The level of another iron-related protein, IscS (PP_0842) cysteine desulfurase, involved in providing sulfur for iron-sulfur cluster assembly, was increased. This suggests that Co could exert its toxicity as an iron competitor, leading to the inactivation of iron-sulfur cluster-containing proteins as previously established.¹¹

Others. The synthesis of nucleotides could be also affected. Proteins involved in the inosine-5'-phosphate (IMP) *de novo* biosynthesis pathway and the following adenosine nucleotide *de novo* pathway were both affected after exposure to not only Co but also Ni. Indeed PurT (PP_1457) (Table 1), PurC (PP_1240) and PurB (PP_4016) (Table 3), and PurA (PP_4889) (Table 2) displayed decreased levels. This pathway leads to the formation of IMP, which is converted to ADP *via* the action of

Table 3 Differentially expressed proteins identified in *P. putida* KT2440 that were regulated by both Co and Ni treatments

Spot number	Ni/ Ctrl	Co/ Ctrl	Accession no	Protein (gene) [EC]	Functional classification	PI	MW, kDa
118	0.46	0.10	PP_0011	DNA polymerase III, beta subunit (<i>dnaN</i>) [2.7.7.7]	Cell growth/division	5	40.7
10	0.24	0.29	PP_4378	Flagellin flhC (<i>flhC</i>)	Cell structure: motility	4.39	67.80
362	1.78	6.75	PP_3587	Thiol peroxidase (<i>tpx</i>) [1.11.1.-]	Antioxidants, detoxification	4.99	17.6
203	5.01	1.88	PP_4506	Nitroreductase family protein	Antioxidants, detoxification	6.16	20.0
270–297	1.76	3.73	PP_1084	Alkyl hydroperoxide reductase, AhpC/Tsa family	Antioxidants, detoxification	5.06	21.9
52	2.40	4.94	PP_2463	Cold shock protein CspA (<i>cspA-2</i>)	Antioxidants, detoxification	6.56	7.7
44	0.23	0.52	PP_0336	Peptide methionine sulfoxide reductase (<i>msrA</i>) [1.8.4.6]	Antioxidants, detoxification	—	—
196	0.37	0.23	PP_2132	Universal stress protein family UspA	Antioxidants, detoxification	6.14	16.4
332	5.69	4.46	PP_5414	ATP synthase F1, gamma subunit (<i>atpG</i>) [3.6.3.14]	Energy	9.5	31.4
222	0.21	0.11	PP_5413	ATP synthase F1, beta subunit (<i>atpD</i>) [3.6.3.14]	Energy	4.88	49.4
18_107	0.33	0.20	PP_4116	Isocitrate lyase (<i>aceA</i>) [4.1.3.1]	Energy: glyoxylate cycle	5.38	48.6
239	0.26	0.17	PP_4965	Transketolase (<i>tktA</i>) [2.2.1.1]	Energy: pentose phosphate pathway	5.2	72.8
552	3.53	6.22	PP_0339	Pyruvate dehydrogenase, E1 component (<i>aceE</i>) [1.2.4.1]	Energy: TCA pathway	5.56	99.7
393_567	2.00	1.67	PP_2339	Aconitate hydratase 2 (<i>acnB</i>) [4.2.1.3]	Energy: TCA pathway	5.18	94.2
105	0.49	0.36	PP_4011	Isocitrate dehydrogenase, NADP-dependent, prokaryotic type (<i>icd</i>) [1.1.1.42]	Energy: TCA pathway	5.4	45.7
65	0.40	0.27	PP_4185	Succinyl-CoA synthetase, alpha subunit (<i>sucD</i>) [6.2.1.5]	Energy: TCA pathway	5.89	30.1
285	0.45	0.24	PP_4194	Citrate synthase (<i>glta</i>) [4.1.3.7]	Energy: TCA pathway	6.5	47.9
259	0.33	0.30	PP_1304	Sulfate adenylyltransferase, subunit 1/adenylylsulfate kinase (<i>cysNC</i>) [2.7.7.4]	Metabolism: energy/amino acids/nucleotides	5.51	69.2
163	0.33	0.37	PP_0432	<i>N</i> -Acetylglutamate semialdehyde dehydrogenase (<i>argC1</i>) [1.2.1.38]	Metabolism: amino acids	6.3	36.3
78	0.29	0.28	PP_1000	Ornithine carbamoyltransferase, catabolic (<i>argI</i>) [2.1.3.3]	Metabolism: amino acids	5.92	37.9
106	0.45	0.20	PP_1001	Arginine deiminase (<i>arcA</i>) [3.5.3.6]	Metabolism: amino acids	5.5	46.4
28	0.23	0.42	PP_1988	3-Isopropylmalate dehydrogenase (<i>leuB</i>) [1.1.1.85]	Metabolism: amino acids	5.03	38.9
149	0.28	0.40	PP_2528	<i>O</i> -acetylhomoserine sulfhydrylase (<i>metY</i>) [2.3.1.31]	Metabolism: amino acids	6	45.2
135	0.20	0.21	PP_4223	Diaminobutyrate-2-oxoglutarate transaminase [2.6.1.76]	Metabolism: amino acids	6.54	48.8
236	0.31	0.35	PP_4477	<i>N</i> -succinylarginine dihydrolase (<i>astB</i>)	Metabolism: amino acids	6.03	49.2
122	0.11	0.31	PP_4667	Methylmalonate semialdehyde dehydrogenase (<i>mmsA2</i>) [1.2.1.27]	Metabolism: amino acids	5.7	54.3
14	0.28	0.19	PP_5046	Glutamine synthetase, type I (<i>glnA</i>) [6.3.1.2]	Metabolism: amino acids	5.21	51.7
40	0.18	0.26	PP_5095	Delta-1 pyrroline-5-carboxylate reductase (<i>proC</i>) [1.5.1.2]	Metabolism: amino acids	4.98	28.2
67	0.05	0.12	PP_5289	Acetylglutamate kinase (<i>argB</i>) [2.7.2.8]	Metabolism: amino acids	5.57	31.9
129	0.47	0.19	PP_5338	Aspartate ammonia-lyase (<i>aspA</i>) [4.3.1.1]	Metabolism: amino acids	5.68	51.5
208	2.39	1.60	PP_4869	NH(3)-dependent NAD(+) synthetase (<i>nadE</i>) [6.3.5.1]	Metabolism: cofactors	5.52	29.4
62	0.46	0.29	PP_5104	Thiazole synthase (<i>thiG</i>)	Metabolism: cofactors	5.74	29.2
123	0.23	0.30	PP_0763	Medium-chain-fatty-acid CoA ligase	Metabolism: lipid and sterol	5.47	62.1
74	0.53	0.33	PP_2217	Enoyl-CoA hydratase/isomerase FadB1x (<i>fadB1x</i>)	Metabolism: lipid and sterol	5.43	27.7
73	0.19	0.33	PP_1240	Phosphoribosylaminoimidazole-succinocarboxamide synthase (<i>purC</i>) [6.3.2.6]	Metabolism: nucleotides	5.37	26.9
127	0.41	0.26	PP_4016	Adenylosuccinate lyase (<i>purB</i>) [4.3.2.2]	Metabolism: nucleotides	5.69	50.5
242	0.18	0.18	PP_4179	Heat shock protein HtpG (<i>htpG</i>)	Protein destination and storage: folding and stability	5.21	71.5
386	2.51	1.69	PP_2017	Aminopeptidase N (<i>pepN</i>) [3.4.11.2]	Protein destination and storage: proteolysis	4.9	99.5
58	0.11	0.09	PP_2300	ATP-dependent Clp protease, proteolytic subunit ClpP (<i>clpP</i>) [3.4.21.92]	Protein destination and storage: proteolysis	5.53	23.5
177	2.41	4.95	PP_0444	Ribosomal protein L1 (<i>rplA</i>)	Protein synthesis: ribosomal proteins	9.5	24.2
272	4.22	7.28	PP_0721	Ribosomal 5S rRNA E-loop binding protein Ctc/L25/TL5	Protein synthesis: ribosomal proteins	6	23.3
7	1.91	2.25	PP_1772	Ribosomal protein S1 (<i>rpsA</i>)	Protein synthesis: ribosomal proteins	4.83	63.5
23	1.67	4.12	PP_0440	Translation elongation factor Tu (<i>tuf-1</i>)	Protein synthesis: translation factors	5.22	43.8
43	1.29	2.16	PP_1858	Translation elongation factor P (<i>efp</i>)	Protein synthesis: translation factors	4.73	21.3
219	0.29	0.37	PP_0061	Glycyl-tRNA synthetase, tetrameric type, alpha subunit (<i>glyQ</i>) [6.1.1.14]	Protein synthesis: tRNA synthetases	5	36.1
50	0.23	0.20	PP_4722	Transcription elongation factor GreA (<i>greA</i>)	Transcription: specific TFs	4.85	17.6
167	1.69	2.53	PP_1071	Amino acid ABC transporter, periplasmic amino acid-binding protein	Transporters: ABC type	8.61	33.4
31	0.38	0.11	PP_0282	Amino acid ABC transporter, periplasmic amino acid-binding protein	Transporters: ABC type	5.46	27.9
502	2.66	3.26	PP_3828	Molybdate ABC transporter, periplasmic molybdate-binding protein (<i>modA</i>)	Transporters: ABC type	9	27.0
102	0.47	0.39	PP_5196	Iron ABC transporter, periplasmic iron-binding protein, putative	Transporters: ABC type	5.6	36.8
69	0.17	0.32	PP_0711	Isochorismatase hydrolase	Unclear classification	5.43	23.0
200	3.03	1.46	PP_4981	YceI family protein	Unknown function	7.89	22.1
256	0.43	0.33	PP_4448	Hypothetical protein	Unknown function	5.74	66.5

PurA (PP_4889) and PurB (PP_4016). In *E. coli*, *purA*, *purB*, *purC* and *purE* are under the negative transcriptional control of PurR, the purine nucleotide biosynthesis repressor, which controls its own expression as well.³¹ Interestingly, Fur DNA-binding sites are present in the promoter region of the *purR* gene that links the purine metabolism to the metal metabolism.

Finally, the effect of Co on the stability of mRNAs can be hypothesized. The synthesis of RraA, ribonuclease E inhibitor protein A (PP_2084), decreased. This protein inhibits the activity of RNaseE that plays a central role in mRNA decay, the processing of tRNA, the tmRNA-mediated mRNA quality control.³² RraA binds to RNaseE and inhibits its activity leading to a global change in the half-life and abundance of mRNAs.³³ Down-regulation of RraA is thus expected to increase RNA decay by RNaseE. In *E. coli*, overproduction of RraA affected mRNA levels more notably involved in anaerobic metabolism and cell envelope biosynthesis. Another RNaseE interacting protein is Pnp, poly RNA nucleotidyltransferase (PP_4708). Pnp is involved in mRNA degradation by hydrolyzing single-stranded polyribonucleotides from 3' to 5' and is part of the RNA degradosome.³⁴ Pnp can also function alone in the degradation of small RNAs. In *E. coli* it has been shown that Pnp plays a role for instance in the control of outer membrane protein (OMP) levels.³⁵

The specific response to nickel

Amino acids metabolism. The most prominent response to Ni treatment was the adaptation of amino-acids metabolism (Table 2). We have seen above that glutamate formation seems to be favored in Ni- and Co- treated samples. This is even more pronounced for Ni with the strong increase of glutamate dehydrogenase GdhA (PP_0675) that converts α -ketoglutarate to glutamate. Ni also modified the branched chain amino-acids biosynthesis through the accumulation of the following enzymes. The conversion of pyruvate into 2-oxoisovalerate is carried out by IlvB (PP_4680) and IlvC (PP_4678). The transamination of 2-oxoisovalerate by IlvE (PP_3511) leads to L-valine formation. In contrast, the level of LeuB (PP_1988) (Table 3), participating in the conversion of 2-oxoisovalerate to 4-methyl-2-oxopentionate and then to L-leucine *via* IlvE, was decreased. Interestingly, IlvBC and LeuB were found less abundant in the Co samples (Tables 1 and 3), suggesting that synthesis of branched chain amino acids is an adaptive response to Ni and Co stress.

Conversion of aspartate to L-lysine *via* dihydrodipicolinate synthase DapA (PP_1237) and conversion of aspartate to L-homoserine *via* aspartokinase LysC (PP_4473) seem to be favored by Ni. The conversion of serine into glycine *via* serine hydroxymethyltransferase GlyA2 (PP_0671) was favored in Ni-treated samples not in Co-ones, but the conversion of 3-phosphoglycerate to serine also increased in Co-treated samples *via* SerA (PP_5155) (Table 1). Finally, the synthesis of cysteine *via* the sulfate assimilation pathway was examined. Conversion of sulfate to adenosine-5'-phosphosulfate (APS) by CysNC (PP_1304) was lowered by both Co and Ni (Table 3). However, the conversion of sulfite to sulfide by CysI (PP_2371) and the condensation of sulfide with O-acetyl-L-serine by cysteine synthase (CysK, PP_4571) to yield cysteine were enhanced in Ni-treated samples (Table 2). Quite surprisingly, the level of these

Table 4 Quantification of the expression of genes involved in the response to oxidative stress. Quantification of the expression of the genes was performed by qRT-PCR after growth of the bacteria until the late-log phase in M63 + 0.4% succinate, amended with 75 μ M NiSO₄ (Ni) or 35 μ M CoCl₂ (Co). Expression ratios are relative to the data obtained with the cells grown in M63 + 0.4% succinate. Data are the mean of at least three independent experiments. SDs are presented in brackets

Gene	Protein	Ratio	
		Ni	Co
<i>sodB</i>	Superoxide dismutase	15.7 (0.5)	45.3 (0.4)
<i>trxB</i>	Thioredoxin reductase	-2.5 (0.1)	4.2 (2.2)
<i>trx2</i>	Thioredoxin	1.3 (0.4)	1.9 (0.1)
<i>ohr</i>	Organic hydroperoxide resistance protein	1.1 (0.1)	1.8 (0.3)
<i>tpx</i>	Thiol peroxidase	1.4 (0.0)	7.6 (0.3)

enzymes was reduced by Co (Table 1) suggesting that cysteine biosynthesis could not be supported by sulfate assimilation. Rather it could result from the conversion of cysteinylglycine into L-Cys and Gly *via* aminopeptidase PepN (PP_2017). Indeed, the level of PepN increased in Co and Ni samples (Table 3).

Transporters. In this study, the soluble proteome of *P. putida* was analyzed and transporter proteins were not identified, as they are membrane bound. The exception consists of Periplasmic Binding Proteins (PBP) of the ABC transporter family that are soluble proteins. Several PBPs were modified upon Ni treatment (Table 2). Predicted substrates for these transporters are either ions or amino acids, it is however not possible to assign a precise substrate based only on sequence annotation.

Quantification of the oxidative stress response at the mRNA level

The proteomic data revealed that the effect of Co on cellular stress leads to the accumulation of several proteins involved in the detoxification of peroxides (thioredoxin reductase, thioredoxin, organic hydroperoxide resistance protein and thiol peroxidase) as well as detoxification of superoxides (superoxide dismutase SodB). Concerning the effect of Ni, the effect on oxidative stress was less clear at the protein level. To address the involvement of defense mechanisms towards oxidative stress, the level of expression of the genes encoding the above-mentioned proteins was measured in samples prepared under the same conditions as the ones used for the proteomic analysis.

In the presence of Co, *ohr* encoding organic hydroperoxide resistance protein and *tpx* encoding thiol peroxidase were up-regulated, indicating that under these conditions organic peroxides accumulate in the cell (Table 4). Similarly, the increase of *trxB* (thioredoxin reductase) and *trx2* (thioredoxin) indicates the need for the cell to reduce oxidized thiols that can arise from the oxidation of peroxiredoxins or the direct damage of thiol-containing proteins.³⁶ Finally, the most induced gene was *sodB* encoding superoxide dismutase. This enzyme is involved in the scavenging of superoxide ions to prevent their oxidative deleterious effect.³⁷

Interestingly, the situation in the presence of Ni was different. Indeed, *trx2*, *ohr* and *tpx* were only very slightly induced, and *trxB* was even repressed (Table 4). These regulations suggest that Ni, in contrast to Co, does not cause the apparition of peroxides and that thiol-damage is not more pronounced than under the

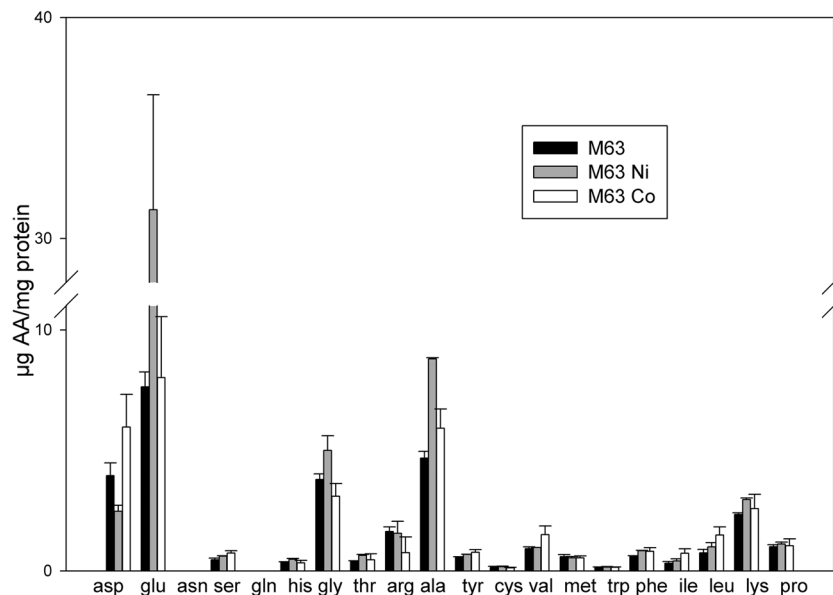


Fig. 4 Concentrations of amino acids present in treated bacteria. The amount of amino acids was measured in whole cells after growth in 0.4% succinate M63 medium (black bars), in the same medium supplemented with 75 μM NiCl_2 (grey bars) or 35 μM CoCl_2 (white bars). The results are expressed in μg of amino acid per mg of total protein. Error bars indicate standard deviations.

control conditions. Still, oxidative stress is present in the Ni-treated samples as *sodB*, encoding superoxide dismutase, was strongly up-regulated, indicating the presence of superoxide radicals.

Modification of the amino acid pools by the addition of Ni or Co

The proteomics data revealed that the expression of a large set of proteins involved in amino acid biosynthesis was modified upon the addition of Ni or Co. This suggests that the level of amino acids might be changed upon the addition of these two metals. To assess the possible effect of these metals on the cellular pools of amino acids, their level in bacteria was assayed after growth either in minimal medium supplemented with 0.4% succinate or in the same medium supplemented with 75 μM NiCl_2 or 35 μM CoCl_2 . In the absence of metal, the most abundant amino acids were glutamate (7.63 μg per mg of total protein), alanine (4.68 μg per mg of total protein), aspartate (3.95 μg per mg of total protein) and glycine (3.79 μg per mg of total protein) (Fig. 4). In the presence of Co, the level of serine increased 1.6 fold and the levels of branched chain amino acids valine, isoleucine and leucine increased twice, while the amount of arginine decreased twice (Fig. 4). It was previously reported that, in *E. coli*, the level of branched chain amino acids increased under paraquat-induced oxidative stress³⁸ and in a tellurite-hyperresistant strain.³⁹ A role for these amino acids in the defense against oxidative stress was thus proposed. In the presence of Ni, the level of alanine increased twice, the levels of isoleucine and leucine increased 1.3 fold while the level of aspartate decreased 1.6 fold. However, very striking was the level of glutamate that increased by a four-fold ratio (Fig. 4). Glutamate plays many roles in the cell. It can be converted to citric acid intermediates to provide energy for the cell. However, synthesis of proteins involved in this conversion was found to be reduced in this study (see above). Moreover, as glutamate

accumulates here, its role as a precursor is not likely. Glutamate was also shown to enhance the stability of several proteins.⁴⁰ Increased levels of glutamate might also reflect the adaptive response of cells to an increase of the osmolarity of the medium.⁴¹ It was shown that accumulation of glutamate has an effect on the transcription of several *E. coli* genes by acting differentially on RNA polymerase.⁴² The data of amino acid amounts measured here are in agreement with the proteomic data and this confirms that the amino acids play a role in the bacterial adaptation to noxious conditions caused by excess concentrations of Ni or Co.

Concluding remarks

This study, by reason of a large number of proteins (160) that were identified and whose accumulation level was quantified, allowed us to perform a thorough investigation of the bacterial cell response to Ni or Co toxicity. The concentrations of these two metals we used influence the bacterial growth and this effect is obvious at the protein level where accumulation of components of the protein synthesis machinery was observed, suggesting the requirement for the cell to repair damaged macromolecules. We also observed a decrease in the level of proteins involved in the central metabolism or amino-acids metabolism. In the Co treated samples, several proteins involved in the defense against oxidative stress were shown to accumulate. Most of the anti-oxidant systems identified participate in the cellular thiol-disulfide homeostasis but interestingly, we also found proteins, such as superoxide dismutase, which are required for the detoxification of ROS. These data argue strongly in favor of Co causing the apparition of ROS, which is considered as controversial in the literature. These results were fully confirmed at the transcriptional level by the up-regulation of genes involved in the detoxification of superoxide radicals,

peroxides and in maintaining the thiol-disulfide homeostasis. These observations were not retrieved in the Ni-treated samples, even if response to oxidative stress was also noticed at the protein level and was confirmed at the RNA level where *sodB*, encoding superoxide dismutase, was strongly up-regulated, indicating that Ni causes the apparition of superoxide radicals. This effect has never been described in the literature yet, however the mechanism by which superoxide ions appear is still to be uncovered. The superoxide radicals are known to damage iron-sulfur cluster containing enzymes leading to the release of iron that in turn can produce ROS through the Fenton reaction.³⁷ The main signature of the effect of Ni was the accumulation of proteins involved in the biosynthesis of amino acids, more particularly, proteins involved in the synthesis of glutamate. When directly assayed in the Ni treated samples, the level of several amino acids changed, the most striking result being the increased accumulation of glutamate, a compound that plays a crucial role in cell survival. Further work is needed to decipher the precise role of amino acids in the defense against Ni toxicity.

Acknowledgements

This work was supported by IFCPAR, grant 3709. We thank Floriant Bellvert and the CESN platform, UCBL, for the amino acids assay. This manuscript is dedicated to the memory of P. Maruthi Mohan, Department of Biochemistry, Osmania University.

References

- 1 Y. Zhang and V. N. Gladyshev, *J. Biol. Chem.*, 2010, **285**, 3393–3405.
- 2 S. B. Mulrooney and R. P. Hausinger, *FEMS Microbiol. Rev.*, 2003, **27**, 239–261.
- 3 M. Kobayashi and S. Shimizu, *Eur. J. Biochem.*, 1999, **261**, 1–9.
- 4 T. Eitinger, J. Suhr, L. Moore and J. A. Smith, *Biometals*, 2005, **18**, 399–405.
- 5 D. Nies, *FEMS Microbiol. Rev.*, 2003, **27**, 313–339.
- 6 A. Rodrigue, G. Effantin and M. A. Mandrand-Berthelot, *J. Bacteriol.*, 2005, **187**, 2912–2916.
- 7 Z. L. He, X. E. Yang and P. J. Stoffella, *J. Trace Elem. Med. Biol.*, 2005, **19**, 125–140.
- 8 S. Smith, *Environ. Int.*, 2009, **35**, 142–156.
- 9 D. Canovas, I. Cases and V. de Lorenzo, *Environ. Microbiol.*, 2003, **5**, 1242–1256.
- 10 A. Haritha, A. Rodrigue and P. M. Mohan, *BMC Res. Notes*, 2008, **1**, 88.
- 11 F. Barras and M. Fontecave, *Metallomics*, 2011, **3**, 1130–1134.
- 12 J. Catusse, J. M. Strub, C. Job, A. Van Dorsselaer and D. Job, *Proc. Natl. Acad. Sci. U. S. A.*, 2008, **105**, 10262–10267.
- 13 A. Shevchenko, M. Wilm, O. Vorm and M. Mann, *Anal. Chem.*, 1996, **68**, 850–858.
- 14 C. Deytieux, L. Geny, D. Lapaillerie, S. Claverol, M. Bonneu and B. Doneche, *J. Exp. Bot.*, 2007, **58**, 1851–1862.
- 15 J. W. Henderson, R. D. Ricker, B. A. Bidlingmeyer and C. Woodward, *Agilent application note*, 2000.
- 16 M. W. Pfaffl, *Nucleic Acids Res.*, 2001, **29**, e45.
- 17 Z. A. Wood, E. Schroder, J. Robin Harris and L. B. Poole, *Trends Biochem. Sci.*, 2003, **28**, 32–40.
- 18 D. F. Ackerley, C. F. Gonzalez, M. Keyhan, R. Blake and A. Matin, *Environ. Microbiol.*, 2004, **6**, 851–860.
- 19 G. Horn, R. Hofweber, W. Kremer and H. Kalbitzer, *Cell. Mol. Life Sci.*, 2007, **64**, 1457–1470.
- 20 C. Loepfe, E. Raimann, R. Stephan and T. Tasara, *Foodborne Pathog. Dis.*, 2010, **7**, 775–783.
- 21 K. E. Nelson, C. Weinel, I. T. Paulsen, R. J. Dodson, H. Hilbert, V. A. P. Martins dos Santos, D. E. Fouts, S. R. Gill, M. Pop, M. Holmes, L. Brinkac, M. Beanan, R. T. DeBoy, S. Daugherty, J. Kolonay, R. Madupu, W. Nelson, O. White, J. Peterson, H. Khouri, I. Hance, P. C. Lee, E. Holtzapple, D. Scanlan, K. Tran, A. Moazzez, T. Utterback, M. Rizzo, K. Lee, D. Kosack, D. Moestl, H. Wedler, J. Lauber, D. Stjepandic, J. Hoheisel, M. Straetz, S. Heim, C. Kiewitz, J. Eisen, K. N. Timmis, A. Düsterhöft, B. Tümmeler and C. M. Fraser, *Environ. Microbiol.*, 2002, **4**, 799–808.
- 22 J. J. Harrison, V. Tremaroli, M. A. Stan, C. S. Chan, C. Vacchi-Suzzi, B. J. Heyne, M. R. Parsek, H. Ceri and R. J. Turner, *Environ. Microbiol.*, 2009, **11**, 2491–2509.
- 23 Z. Cheng, Y. Y. Wei, W. W. Sung, B. R. Glick and B. J. McConkey, *Proteome Sci.*, 2009, **7**, 18.
- 24 M. A. Molina-Henares, J. De La Torre, A. García-Salamanca, A. J. Molina-Henares, M. C. Herrera, J. L. Ramos and E. Duque, *Environ. Microbiol.*, 2010, **12**, 1468–1485.
- 25 C. Tricot, V. Stalon and C. Legrain, *J. Gen. Microbiol.*, 1991, **137**, 2911–2918.
- 26 Y. Meyer, B. B. Buchanan, F. Vignols and J.-P. Reichheld, *Annu. Rev. Genet.*, 2009, **43**, 335–367.
- 27 S. Yeom, J. Yeom and W. Park, *Microbiology*, 2010, **156**, 1487–1496.
- 28 J. A. Dubbs and S. Mongkolsuk, *Subcell. Biochem.*, 2007, **44**, 143–193.
- 29 S. Nair and S. E. Finkel, *J. Bacteriol.*, 2004, **186**, 4192–4198.
- 30 J. R. Fantino, B. Py, M. Fontecave and F. Barras, *Environ. Microbiol.*, 2010, **12**, 2846–2857.
- 31 K. Y. Choi and H. Zalkin, *J. Bacteriol.*, 1992, **174**, 6207–6214.
- 32 D. A. Steege, *RNA*, 2000, **6**, 1079–1090.
- 33 K. Lee, X. Zhan, J. Gao, J. Qiu, Y. Feng, R. Meganathan, S. N. Cohen and G. Georgiou, *Cell*, 2003, **114**, 623–634.
- 34 V. Kaberdin, D. Singh and S. Lin-Chao, *J. Biomed. Sci.*, 2011, **18**, 23.
- 35 J. M. Andrade and C. I. M. Arraiano, *RNA*, 2008, **14**, 543–551.
- 36 B. D'Autreaux and M. B. Toledano, *Nat. Rev. Mol. Cell Biol.*, 2007, **8**, 813–824.
- 37 J. A. Imlay, *Annu. Rev. Biochem.*, 2008, **77**, 755–776.
- 38 H. Tweeddale, L. Notley-McRobb and T. Ferenci, *Redox Rep.*, 1999, **4**, 237–241.
- 39 V. Tremaroli, M. L. Workentine, A. M. Weljie, H. J. Vogel, H. Ceri, C. Viti, E. Tatti, P. Zhang, A. P. Hynes, R. J. Turner and D. Zannoni, *Appl. Environ. Microbiol.*, 2009, **75**, 719–728.
- 40 A. K. Mandal, S. Samaddar, R. Banerjee, S. Lahiri, A. Bhattacharyya and S. Roy, *J. Biol. Chem.*, 2003, **278**, 36077–36084.
- 41 L. N. Csonka, *Microbiol. Rev.*, 1989, **53**, 121–147.
- 42 J. D. Gralla and D. R. Vargias, *EMBO J.*, 2006, **25**, 1515–1521.